

Journal of Biomedical Optics

SPIDigitalLibrary.org/jbo

Extraction of effective parameters of anisotropic optical materials using a decoupled analytical method

Thi-Thu-Hien Pham
Yu-Lung Lo



SPIE

Extraction of effective parameters of anisotropic optical materials using a decoupled analytical method

Thi-Thu-Hien Pham^a and Yu-Lung Lo^{a,b}

^aNational Cheng Kung University, Department of Mechanical Engineering, Tainan 701, Taiwan

^bNational Cheng Kung University, Advanced Optoelectronic Technology Center, Tainan 701, Taiwan

Abstract. A decoupled analytical technique based on the Mueller matrix method and the Stokes parameters is proposed for extracting effective parameters of anisotropic optical materials in linear birefringence (LB), linear dichroism (LD), circular birefringence (CB), and circular dichroism (CD) properties. This technique is essential in determining the optical properties of opto-electric or biomedical materials for the development of advanced inspection and/or diagnostic applications. The error and resolution analysis of the proposed approach is demonstrated by extracting the effective parameters given an assumption of errors ranging ± 0.005 in the values of the output Stokes parameters. The results confirm the ability of the proposed method to yield full-range measurements of all the optical parameters. The decoupled nature of the analytical model yields several important advantages, including an improved accuracy and the ability to extract the parameters of optical samples with only LB, CB, LD, or CD property without using compensation technique or pretreatment. Moreover, by decoupling the extraction process, the "multiple solutions" problem inherent in previous models presented by the current group is avoided. © 2012 Society of Photo-Optical Instrumentation Engineers (SPIE). [DOI: 10.1117/1.JBO.17.2.025006]

Keywords: dichroism; birefringence; polarimetry; Mueller matrix; Stokes polarimeter.

Paper 11365 received Jul. 12, 2011; revised manuscript received Nov. 18, 2011; accepted for publication Dec. 12, 2011; published online Mar. 12, 2012.

1 Introduction

Methods for accurately determining the optical properties of opto-electric materials or biosamples are essential in facilitating the development of advanced inspection and/or diagnostic applications. For example, linear birefringence (LB) measurements provide a useful insight into the characteristics of liquid crystal display (LCD) compensator films or the photo-elasticity of human tissue, while circular birefringence (CB) measurements of human blood provide a reliable indication of diabetes. Similarly, linear dichroism (LD) measurements of human tissue can facilitate tumor diagnosis, while circular dichroism (CD) measurements are an effective means of characterizing and classifying protein structures.¹⁻²⁶

CD analyses provide a reliable means of classifying different proteins.²⁻⁵ In addition, CD spectroscopy is also extensively used to probe a wide range of optically active (chiral) materials, ranging from small molecules to macromolecules.⁶⁻⁸ For example, Kuroda et al.⁹ designed and constructed a CD spectrophotometer (USC-1: J-800KCM) featuring a special sample holder designed to eliminate the parasitic artifacts caused by macroscopic anisotropies, such as LB and LD, that are unique to solid state samples. In a later study,¹⁰ the same group presented a universal chiroptical spectrophotometer (UCS-2: J-800KCMF) for the in-situ chirality measurement of solid samples. As in the spectrophotometer proposed in Kuroda et al.,⁹ the artifact signals arising from macroscopic anisotropies unique to the solid state were removed using two lock-in amplifiers. The effectiveness of the proposed device was demonstrated by measuring the microcrystallines of both enantiomers of ammonium camphorsulfonate. However, while

the spectrophotometer was capable of measuring both the CD and the CB properties of anisotropic optical samples, the Mueller matrix formulations used to extract the optical parameters were not decoupled. As a result, the device was restricted to samples with pure CD properties only or pure CB properties only.

Asahi and Kobayashi^{11,12} proposed an ellipsometry method using the general high accuracy universal polarimeter (HAUP) theory for determining the LB/CB and LD/CD of an anisotropic optically active material. The experimental results of the proposed approach showed gyration tensor components in various samples, such as BaMnF₄, poly-L-lactic acids, lysozyme crystal, and silver thiogallate. However, the basic assumption in HAUP theory requires the principal birefringence axis and diattenuation axis to be aligned. Kaminsky et al.¹³⁻¹⁵ extracted the LB, LD, CB, and CD properties of crystals using a polarimetric imaging technique and an analytical model based on a Jones calculus formulation. However, in characterizing the samples, different tools were used for each optical property. For example, the LB and LD properties were extracted using a Metripol microscope, while the CB properties were analyzed using a HAUP or Scanning-HAUP, and the CD properties were examined using a circular dichroism imaging microscope. As a result, the optical parameters were not decoupled in the analytical model. That is, in extracting each optical property, the knowledge of one or more of the other properties was required. Consequently, the precision of the extraction results was highly sensitive to the effects of accumulated errors.

In addition, Chenault and Chipman¹⁶⁻¹⁹ proposed a technique for measuring the LD and LB spectra of infrared solid materials in transmission based on the Mueller matrix decomposition method. In the proposed approach, the intensity of the detected

Address all correspondence to: Yu-Lung Lo, National Cheng Kung University, Department of Mechanical Engineering, Tainan 701, Taiwan. Tel: +886 6 2757575x62100; Fax: +886 6 2352973; E-mail: loyl@mail.ncku.edu.tw

signal was modulated by rotating the sample, and the LD and LB properties were calculated from the Fourier series coefficients of the detected signal at each wavelength. However, in extracting the sample parameters, an assumption was made that the principal birefringence axis and diattenuation axis were aligned. Ghosh et al.²⁰⁻²³ proposed a method using a Mueller matrix decomposition method to extract the polarization properties (linear retardance, optical rotation angle, diattenuation, and depolarization coefficient) of a complex turbid media. In the experimental studies, a photoelastic modulation polarimeter was used to record Mueller matrices from polyacrylamide phantoms having strain-induced birefringence, sucrose-induced optical activity, and polystyrene microspheres-induced scattering. Wang and his group²⁴ also presented comparisons of Mueller matrix elements of light backscattering from birefringent anisotropic turbid media containing glucose in single-scattering model and a double-scattering model with the Monte Carlo model. Huang and Knighton^{25,26} proposed a method to measure the diattenuation spectrum and the birefringence of the isolated rat retinal nerve fiber layer (RNFL) for glaucoma diagnosis using scanning laser polarimetry at wavelengths from 440 to 830 nm. The degree of polarization for reflection from the RNFL was also measured. It is noted that the above studies²⁰⁻²⁶ were based on the Mueller matrix method; studies by Ghosh et al. and Wood et al.²⁰⁻²³ were based on the Mueller matrix polar decomposition method in Lu and Chipman.²⁷ Additionally, differential matrix formalism for an anisotropic medium in parallelism with Jones' matrix formalism was proposed by Azzam.²⁸ Ossikovski²⁹ extended the differential matrix formalism including depolarizing media. Ortega-Quijano and Arce-Diego^{30,31} also proposed the differential Mueller matrices for general depolarizing media for measurements in transmission and backward direction.

Recently, Chen et al.³² proposed a technique for measuring the effective LB and LD properties of an optical sample using an analytical model based on the Mueller matrix and the Stokes parameter. More recently, the same group extended the proposed technique to measure the effective LB, LD, and CB properties of an optical fiber for designing an optical fiber-type polarimeter.³³ However, in both studies,^{32,33} a "multiple solutions" problem was observed for samples with a LD value, D , close to one. That is, for samples with $D \approx 1$, both the orientation angle and phase retardance of LB in^{32,33} varied randomly with changes in the orientation angle of LD. Moreover, in both analytical

models, the LB and CB properties of the sample were not decoupled, and thus the accuracy of the LB measurements was highly sensitive to errors in the CB measurements, and vice versa.

The present study proposes a new decoupled analytical technique based on the Mueller matrix method and the Stokes parameters for extracting the orientation angle of fast axis and phase retardance of LB, orientation angle and linear dichroism of LD, optical rotation of CB, and circular dichroism of CD of anisotropic optical materials without considering the scattering factor. Moreover, the decoupled nature of the analytical model localizes the effects of measurement errors and provides the means to extract the parameters of optical samples with only LB, CD, LD, or CB properties. The validity of the proposed approach is demonstrated by extracting the effective parameters of six optical samples. Moreover, de-ionized water containing D-glucose is chosen to evaluate the performance of the proposed method in measuring CB. It is shown that the analytical model yields accurate results even when the output Stokes parameters have errors in the range of ± 0.005 or the samples have very low values of birefringence or dichroism.

2 Analytical Technique for Extracting Effective Optical Parameters of Anisotropic Materials

This section presents the proposed analytical technique for determining the effective LB, LD, CB, and CD properties of anisotropic optical materials. Note that the depolarization (i.e., scattering) properties of the optical material are not considered in this study. Also, in developing an optically equivalent model of the anisotropic material, it is assumed that the CD and LD components of the sample are positioned in front of the CB and LB components.^{34,35} For the nondepolarizing Mueller matrix, Ossikovski³⁵ proposed that the decomposition allows for a straightforward interpretation and parameterization of an experimentally determined Mueller matrix in terms of an arrangement of polarization devices and their characteristic parameters: diattenuations, retardances, and axis azimuths.

According to Chen et al.,³² Lo et al.,³³ and Savenko et al.,³⁶ the Mueller matrix for a LB material with an orientation angle α and phase retardance β can be expressed as

$$M_{lb} = \begin{pmatrix} 1 & 0 & 0 & 0 \\ 0 & \cos(4\alpha)\sin^2(\beta/2) + \cos^2(\beta/2) & \sin(4\alpha)\sin^2(\beta/2) & -\sin(2\alpha)\sin(\beta) \\ 0 & \sin(4\alpha)\sin^2(\beta/2) & -\cos(4\alpha)\sin^2(\beta/2) + \cos^2(\beta/2) & \cos(2\alpha)\sin(\beta) \\ 0 & \sin(2\alpha)\sin(\beta) & -\cos(2\alpha)\sin(\beta) & \cos(\beta) \end{pmatrix}. \quad (1)$$

The Mueller matrix for a CB material with an optical rotation angle γ can be expressed as

$$M_{cb} = \begin{pmatrix} 1 & 0 & 0 & 0 \\ 0 & \cos(2\gamma) & \sin(2\gamma) & 0 \\ 0 & -\sin(2\gamma) & \cos(2\gamma) & 0 \\ 0 & 0 & 0 & 1 \end{pmatrix}. \quad (2)$$

Meanwhile, the Mueller matrix for a LD material with an orientation angle θ_d and linear dichroism D has the form

$$M_{ld} = \begin{pmatrix} \frac{1}{2} \left(1 + \frac{1-D}{1+D}\right) & \frac{1}{2} \cos(2\theta_d) \left(1 - \frac{1-D}{1+D}\right) & \frac{1}{2} \sin(2\theta_d) \left(1 - \frac{1-D}{1+D}\right) & 0 \\ \frac{1}{2} \cos(2\theta_d) \left(1 - \frac{1-D}{1+D}\right) & \frac{1}{4} \left[\left(1 + \sqrt{\frac{1-D}{1+D}}\right)^2 + \cos(4\theta_d) \left(1 - \sqrt{\frac{1-D}{1+D}}\right)^2 \right] & \frac{1}{4} \sin(4\theta_d) \left(1 - \sqrt{\frac{1-D}{1+D}}\right)^2 & 0 \\ \frac{1}{2} \sin(2\theta_d) \left(1 - \frac{1-D}{1+D}\right) & \frac{1}{4} \sin(4\theta_d) \left(1 - \sqrt{\frac{1-D}{1+D}}\right)^2 & \frac{1}{4} \left[\left(1 + \sqrt{\frac{1-D}{1+D}}\right)^2 - \cos(4\theta_d) \left(1 - \sqrt{\frac{1-D}{1+D}}\right)^2 \right] & 0 \\ 0 & 0 & 0 & \sqrt{\frac{1-D}{1+D}} \end{pmatrix}. \quad (3)$$

Table 1 Symbols and definitions of six effective parameters.^{12,37,38}

Name	Symbol	Range	Definition ^a
Orientation angle of fast axis of LB	α	[0 deg, 180 deg]	
Linear birefringence of LB	β	[0 deg, 360 deg]	$2\pi(n_s - n_f)l/\lambda_0$
Optical rotation of CB	γ	[0 deg, 180 deg]	$2\pi(n_- - n_+)l/\lambda_0$
Orientation angle of LD	θ_d	[0 deg, 180 deg]	
Linear dichroism of LD	D	[0, 1]	$2\pi(\mu_s - \mu_f)l/\lambda_0$
Circular dichroism of CD	R	[-1, 1]	$2\pi(\mu_- - \mu_+)l/\lambda_0$

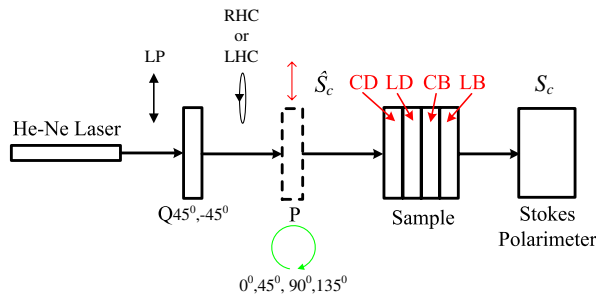
^a n is refractive index, μ is absorption coefficient, l is path length through the medium (thickness of material), λ_0 is vacuum wavelength. Subscripts f and s represent the fast and slow linearly polarized waves when neglecting the circular effects, and $+$ and $-$ the right and left circular polarized waves when neglecting the linear effects.

Finally, the Mueller matrix for a CD material with circular dichroism R has the form

$$M_{cd} = \begin{bmatrix} 1 + R^2 & 0 & 0 & 2R \\ 0 & 1 - R^2 & 0 & 0 \\ 0 & 0 & 1 - R^2 & 0 \\ 2R & 0 & 0 & 1 + R^2 \end{bmatrix}. \quad (4)$$

Note that R is equal to $(r_R - r_L)/(r_R + r_L)$, where r_R and r_L are the absorptions of right- and left-hand circular polarization light, respectively.³⁶ Table 1 presents the symbols and definitions of six effective parameters used in the proposed study.^{12,37,38}

From Eqs. (1)–(4), it follows that to characterize an anisotropic optical material with hybrid properties, it is necessary to extract a total of six effective parameters. Figure 1 presents a


Fig. 1 Schematic illustration of model used to characterize anisotropic material.

schematic illustration of the setup used in the present study to extract these parameters for a typical anisotropic sample. Note that P and Q are a polarizer and quarter-wave plate, respectively, and are used to produce various linear and circular polarization lights, while \hat{S}_c and S_c are the input and output Stokes vectors, respectively.

The output Stokes vector in Fig. 1 can be calculated as

$$S_c = \begin{bmatrix} S_0 \\ S_1 \\ S_2 \\ S_3 \end{bmatrix}_c = [M_{lb}][M_{cb}][M_{ld}][M_{cd}]\hat{S}_c = \begin{pmatrix} m_{11} & m_{12} & m_{13} & m_{14} \\ m_{21} & m_{22} & m_{23} & m_{24} \\ m_{31} & m_{32} & m_{33} & m_{34} \\ m_{41} & m_{42} & m_{43} & m_{44} \end{pmatrix} \begin{pmatrix} \hat{S}_0 \\ \hat{S}_1 \\ \hat{S}_2 \\ \hat{S}_3 \end{pmatrix}_c, \quad (5)$$

where $[M_{ld}]$, $[M_{lb}]$, $[M_{cb}]$, and $[M_{cd}]$ are the Mueller matrices corresponding to the effective LD, LB, CB, and CD properties of the anisotropic sample, respectively. In Eq. (5), elements $m_{11} - m_{44}$ are all non-zero. As a result, solving the Mueller matrix product is highly complex. Accordingly, in the present study, a method is proposed for extracting the effective LD/CD of the sample using only elements m_{11} , m_{12} , m_{13} , and m_{14} . In the setup shown in Fig. 1, the sample is illuminated using six different input polarization lights, namely four linear polarization lights (i.e., $\hat{S}_{0^\circ} = [1, 1, 0, 0]^T$, $\hat{S}_{45^\circ} = [1, 0, 1, 0]^T$, $\hat{S}_{90^\circ} = [1, -1, 0, 0]^T$, and $\hat{S}_{135^\circ} = [1, 0, -1, 0]^T$)

and two circular polarization lights (i.e., right-handed $\hat{S}_{\text{RHC}} = [1, 0, 0, 1]^T$ and left-handed $\hat{S}_{\text{LHC}} = [1, 0, 0, -1]^T$). The corresponding output Stokes vectors are obtained from Eq. (5) as

$$S_0 = \begin{bmatrix} m_{11} + m_{12}, & m_{21} + m_{22}, & m_{31} + m_{32}, & m_{41} + m_{42} \end{bmatrix}^T \quad (6)$$

$$S_{45^\circ} = \begin{bmatrix} m_{11} + m_{13}, & m_{21} + m_{23}, & m_{31} + m_{33}, & m_{41} + m_{43} \end{bmatrix}^T \quad (7)$$

$$S_{90^\circ} = \begin{bmatrix} m_{11} - m_{12}, & m_{21} - m_{22}, & m_{31} - m_{32}, & m_{41} - m_{42} \end{bmatrix}^T \quad (8)$$

$$S_{135^\circ} = \begin{bmatrix} m_{11} - m_{13}, & m_{21} - m_{23}, & m_{31} - m_{33}, & m_{41} - m_{43} \end{bmatrix}^T \quad (9)$$

$$S_{\text{RHC}} = \begin{bmatrix} m_{11} + m_{14}, & m_{21} + m_{24}, & m_{31} + m_{34}, & m_{41} + m_{44} \end{bmatrix}^T \quad (10)$$

$$S_{\text{LHC}} = \begin{bmatrix} m_{11} - m_{14}, & m_{21} - m_{24}, & m_{31} - m_{34}, & m_{41} - m_{44} \end{bmatrix}^T \quad (11)$$

where

$$m_{11} = \frac{1}{2} \left(1 + \frac{1-D}{1+D} \right) (1 + R^2) \quad (12)$$

$$m_{12} = \frac{1}{2} \left(1 - \frac{1-D}{1+D} \right) \cos(2\theta_d) (1 - R^2) \quad (13)$$

$$m_{13} = \frac{1}{2} \left(1 - \frac{1-D}{1+D} \right) \sin(2\theta_d) (1 - R^2) \quad (14)$$

$$m_{14} = \left(1 + \frac{1-D}{1+D} \right) R. \quad (15)$$

From the values of m_{11} , m_{12} , m_{13} , and m_{14} , Eqs. (12)–(15) are then used to obtain the LD and CD properties of the sample. Specifically, the orientation angle (θ_d) of LD is obtained as

$$2\theta_d = \tan^{-1} \left(\frac{S_{45^\circ}(S_0) - S_{135^\circ}(S_0)}{S_{0^\circ}(S_0) - S_{90^\circ}(S_0)} \right). \quad (16)$$

From Eqs. (12)–(15), the linear dichroism (D) is obtained as either

$$D = \frac{\sqrt{\left[S_{0^\circ}(S_0) - S_{90^\circ}(S_0) \right]^2 + \left[S_{45^\circ}(S_0) - S_{135^\circ}(S_0) \right]^2}}{\sqrt{\left[S_{0^\circ}(S_0) + S_{90^\circ}(S_0) \right]^2 - \left[S_{\text{RHC}}(S_0) - S_{\text{LHC}}(S_0) \right]^2}}, \quad (17)$$

or

$$D = \frac{\left[S_{0^\circ}(S_0) - S_{90^\circ}(S_0) \right]}{\cos(2\theta_d) \left[\sqrt{\left[S_{0^\circ}(S_0) + S_{90^\circ}(S_0) \right]^2} - \left[S_{\text{RHC}}(S_0) - S_{\text{LHC}}(S_0) \right]^2 \right]}, \quad (18)$$

or

$$D = \frac{\left[S_{45^\circ}(S_0) - S_{135^\circ}(S_0) \right]}{\sin(2\theta_d) \left[\sqrt{\left[S_{0^\circ}(S_0) + S_{90^\circ}(S_0) \right]^2} - \left[S_{\text{RHC}}(S_0) - S_{\text{LHC}}(S_0) \right]^2 \right]}. \quad (19)$$

Again, the circular dichroism R is obtained as

$$R = \frac{\left[S_{0^\circ}(S_0) + S_{90^\circ}(S_0) \right] - \left[\sqrt{\left[S_{0^\circ}(S_0) + S_{90^\circ}(S_0) \right]^2} - \left[S_{\text{RHC}}(S_0) - S_{\text{LHC}}(S_0) \right]^2 \right]}{\left[S_{\text{RHC}}(S_0) - S_{\text{LHC}}(S_0) \right]}. \quad (20)$$

Significantly, the values of θ_d , D , and R obtained from Eqs. (16), (17), and (20), respectively, are totally decoupled manner. Moreover, for values of θ_d other than 0-deg or 45-deg Eqs. (18) and (19) yield the same theoretical solution, and thus the equality (or otherwise) of the results obtained from the two equations provides the means to check the correctness of the experimental results.

Once the LD and CD properties are known, the product of the linear dichroism and circular dichroism Mueller matrix can be calculated as

$$M_D = [M_{ld}][M_{cd}] = \begin{pmatrix} B_{11} & B_{12} & B_{13} & B_{14} \\ B_{12} & B_{22} & B_{23} & B_{24} \\ B_{13} & B_{23} & B_{33} & B_{34} \\ B_{41} & B_{42} & B_{43} & B_{44} \end{pmatrix}, \quad (21)$$

where $B_{11} - B_{44}$ are all functions of θ_d , D , and R , and can be extracted from Eqs. (16), (17), and (20), respectively. Note

that all of the elements other than B_{42} and B_{43} are non-zero. The Mueller matrix of retardance has the form

$$M_R = [M_{lb}][M_{cb}] = \begin{pmatrix} 1 & A_{12} & A_{13} & A_{14} \\ A_{21} & A_{22} & A_{23} & A_{24} \\ A_{31} & A_{32} & A_{33} & A_{34} \\ A_{41} & A_{42} & A_{43} & A_{44} \end{pmatrix}, \quad (22)$$

where $A_{12} - A_{44}$ are functions of the orientation angle (α) and phase retardance (β) of LB and optical rotation angle (γ) of CB. It is noted that elements A_{12} , A_{13} , A_{14} , A_{21} , A_{31} , and A_{41} are all equal to zero. From Eqs. (21) and (22), it follows that the effective Mueller matrix for the LB, CB, LD, and CD properties of the anisotropic sample can be expressed as

$$M_{RD} = M_R M_D = \begin{pmatrix} B_{11} & B_{12} & B_{13} & B_{14} \\ A_{22}B_{12} + A_{23}B_{13} + A_{24}B_{41} & A_{22}B_{22} + A_{23}B_{23} & A_{22}B_{23} + A_{23}B_{33} & A_{22}B_{24} + A_{23}B_{34} + A_{24}B_{44} \\ A_{32}B_{12} + A_{33}B_{13} + A_{34}B_{41} & A_{32}B_{22} + A_{33}B_{23} & A_{32}B_{23} + A_{33}B_{33} & A_{32}B_{24} + A_{33}B_{34} + A_{34}B_{44} \\ A_{42}B_{12} + A_{43}B_{13} + A_{44}B_{41} & A_{42}B_{22} + A_{43}B_{23} & A_{42}B_{23} + A_{43}B_{33} & A_{42}B_{24} + A_{43}B_{34} + A_{44}B_{44} \end{pmatrix}. \quad (23)$$

It is noted that all of the elements in the effective Mueller matrix [MRD] be obtained from Eqs. (6)–(11) (i.e. from the output Stokes vectors of experiment), while only m_{11} , m_{12} , m_{13} , m_{14} of [MRD] are used to calculate the LD/CD values. In other words, the elements in [MD] and [MRD] can be obtained from Eqs. (6)–(11). Once all of the elements in [MD] and [MRD] are known, those in the Mueller matrix of retardance [MR] can be inversely derived. Once all of the elements in $[M_D]$ and $[M_{RD}]$ are known, those in the Mueller matrix of retardance $[M_R]$ can be inversely derived. It is noted that the elements of Mueller matrix in Eq. (21) can be easily extracted by Eqs. (6)–(11).

In this study, two methods are proposed for calculating the LB and CB properties of an anisotropic optical material. In the first method (the default method), the values of α , β , and γ are derived using elements A_{22} , A_{23} , A_{24} , A_{32} , A_{33} , A_{34} and A_{44} in the Mueller matrix of retardance $[M_R]$. Specifically, the orientation angle of LB is obtained as

$$\alpha = \frac{1}{2} \tan^{-1} \left(-\frac{A_{24}}{A_{34}} \right). \quad (24)$$

Meanwhile, the phase retardance is obtained as either

$$\beta = \tan^{-1} \left(\frac{A_{34}}{\cos(2\alpha)A_{44}} \right), \quad (25)$$

or

$$\beta = \cos^{-1}(A_{44}). \quad (26)$$

The optical rotation angle of CB can be calculated as follows:

$$\gamma = \frac{1}{2} \tan^{-1} \left(\frac{A_{23} - A_{32}}{A_{22} + A_{33}} \right). \quad (27)$$

The equality (or otherwise) of the results obtained for the phase retardance using Eqs. (25) and (26), respectively, provides the means to check the correctness of the experimental results. Once the orientation angle and retardance of LB are known, the other ways to obtain the optical rotation (γ) of CB are expressed as

$$\gamma = \frac{1}{2} \tan^{-1} \left(\frac{-C_2 A_{22} + C_1 A_{23}}{C_1 A_{22} + C_2 A_{23}} \right), \quad (28)$$

or

$$\gamma = \frac{1}{2} \tan^{-1} \left(\frac{-C_3 A_{32} + C_2 A_{33}}{C_2 A_{32} + C_3 A_{33}} \right), \quad (29)$$

where

$$C_1 = \cos(2\alpha)^2 + \cos(\beta) \sin(2\alpha)^2, \quad (30)$$

$$C_2 = \cos(2\alpha)(1 - \cos(\beta)) \sin(2\alpha), \quad (31)$$

$$C_3 = \cos(2\alpha)^2 \cos(\beta) + \sin(2\alpha)^2. \quad (32)$$

The equality of the results obtained for the optical rotation using Eqs. (27)–(29) provides the means to check the correctness of the experimental results.

For optical samples with a linear dichroism close to one ($D \approx 1$), elements B_{41} and B_{44} in the product of the linear/circular dichroism Mueller matrix [Eq. (21)] are close to zero. In other words, the Mueller matrix of $[M_D]$ is a singular matrix. As a result, the Mueller matrix of $[M_R]$ [Eq. (22)] cannot be found. Consequently, the values of the orientation angle, phase retardance and optical rotation of LB/CB in elements

of Mueller matrix [MR] in the first method are unreliable. Therefore, an alternative method is proposed for calculating the LB and CB properties of anisotropic optical samples with high linear dichroism. In the proposed approach, elements of Mueller matrix of retardance [M_R] (except A_{24} , A_{34} and A_{44}) are obtained as:

$$\begin{bmatrix} B_{22} & B_{23} & 0 & 0 & 0 & 0 \\ B_{23} & B_{33} & 0 & 0 & 0 & 0 \\ 0 & 0 & B_{22} & B_{23} & 0 & 0 \\ 0 & 0 & B_{23} & B_{33} & 0 & 0 \\ 0 & 0 & 0 & 0 & B_{22} & B_{23} \\ 0 & 0 & 0 & 0 & B_{23} & B_{33} \end{bmatrix} \begin{bmatrix} A_{22} \\ A_{23} \\ A_{32} \\ A_{33} \\ A_{42} \\ A_{43} \end{bmatrix} = \begin{bmatrix} m_{22} \\ m_{23} \\ m_{32} \\ m_{33} \\ m_{42} \\ m_{43} \end{bmatrix}. \quad (33)$$

Therefore, the optical rotation angle of CB is calculated from elements A_{22} , A_{23} and A_{33} using Eq. (27). Meanwhile, the phase retardance is obtained as

$$\beta = \sin^{-1} \left[-\frac{A_{43}}{\cos(2\alpha + 2\gamma)} \right], \quad (34)$$

where

$$2\alpha + 2\gamma = \tan^{-1} \left(-\frac{A_{42}}{A_{43}} \right). \quad (35)$$

Having extracted the optical rotation angle and phase retardance of the sample, the orientation angle (α) of LB can be obtained as

$$\alpha = \frac{1}{2} \tan^{-1} \left(\frac{C_{11}A_{42} + C_{22}A_{43}}{C_{22}A_{42} - C_{11}A_{43}} \right), \quad (36)$$

where

$$C_{11} = \cos(2\gamma) \sin(\beta), \quad (37)$$

$$C_{22} = \sin(2\gamma) \sin(\beta). \quad (38)$$

In summary, in the decoupled analytical model proposed in this study, the orientation angle (α) and phase retardance (β) of LB, optical rotation (γ) of CB, orientation angle (θ_d) and linear dichroism (D) of LD, and circular dichroism (R) of CD are extracted using Eqs. (24), (26), (27), (16), (17), and (20), respectively. Also, it is noted that Eqs. (24), (26), (27), (16), (17), and (20) can be simplified as only the function of the measured Mueller elements. For samples with a linear dichroism of $D \approx 1$, the optical rotation of CB, phase retardance and orientation angle of LB are extracted using Eqs. (27), (34), and (36), respectively. As a result, the robustness of the extracted results toward experimental measurement errors is reduced and the ‘‘coupling’’ and the ‘‘multiple solutions’’ problems in Chen et al.³² and Lo et al.³³ are resolved. Importantly, the model provides the means to extract the properties of samples with only LB, CB, LD, or CD properties without the need for any form of compensation process. Furthermore, in similar to the models presented in Chen et al.³² and Lo et al.,³³ the proposed methodology does not require the principal birefringence axes and dichroism axes to be aligned.

3 Analytical Simulations and Error Analysis

In this section, the ability of the proposed analytical method to extract the six effective optical parameters over the measurement ranges is verified using a simulation technique. A further series of simulations is then performed to evaluate the accuracy of the results obtained from the proposed method given errors of ± 0.005 in the values of the output Stokes parameters.^{32,33} (Note that the error range defined here is consistent with the measurement precision of a typical commercial polarimeter.) Finally, simulations are performed to investigate the resolution of the proposed method in extracting the properties of anisotropic samples with very low retardance, linear dichroism, optical rotation, and circular dichroism, respectively.

3.1 Analytical Simulations

In performing the analytical simulations, the theoretical values of the output Stokes parameters for the six input lights, namely S_{0° , S_{45° , S_{90° , S_{135° , S_{RHC} , and S_{LHC} , were calculated for a hypothetical sample using the Jones matrix formulation based on given values of the sample parameters and a knowledge of the input Stokes vectors. The theoretical Stokes values were then inserted into the analytical model derived in Sec. 2 in order to derive the effective optical parameters. Finally, the extracted values of the effective optical parameters were compared with the input values used in the Jones matrix formulation.

The ability of the proposed method is evaluated by extracting α , β , θ_d , D , γ , and R of an anisotropic sample, respectively. When a parameter is extracted, the input of this extracted parameter is changed over its full range (i.e., α , θ_d , and γ : 0-deg to 180-deg; β : 0-deg to 360-deg; D : 0 to 1; and R : -1 to 1). The other input parameters were specified as follows: $\alpha = 50$ -deg, $\beta = 60$ -deg, $\theta_d = 35$ -deg, $D = 0.4$, $\gamma = 15$ -deg and $R = 0.1$. For example, to extract the principal axis angle of LB, the orientation angle of LB extracted using Eq. (24) was specified as α : 0-deg to 180-deg and the other input parameters were specified as $\beta = 60$ -deg, $\theta_d = 35$ -deg, $D = 0.4$, $\gamma = 15$ -deg, and $R = 0.1$, respectively.^{32,33} It is found that the proposed model enables the orientation angle of LD in Eq. (16), linear dichroism in Eq. (17), and circular dichroism in Eq. (20) to be measured over the full range. Again, the analytical model proposed in this study enables the full-range measurement of the orientation angle of LB in Eq. (24), phase retardance in Eq. (26), and optical rotation in Eq. (27), respectively. The results confirm the ability of the proposed method to yield full-range measurements of six effective parameters.

3.2 Error Analysis of Proposed Analytical Model

To examine the robustness of the proposed analytical model toward errors in the output Stokes parameter values, the Jones matrix formulation was used to derive the theoretical output Stokes parameters S_{0° , S_{45° , S_{90° , S_{135° , S_{RHC} , and S_{LHC} for a composite sample with given LB/CB/LD/CD properties and known input polarization states. The 500 sets of error-affected Stokes parameters were then produced by applying random perturbations around ± 0.005 to the theoretical Stokes parameters.^{32,33} The perturbed Stokes parameter values were then inserted into the analytical model in order to extract the effective parameters of the sample. Finally, the extracted values of the optical properties were compared with the given values used in the Jones matrix formulation.

Table 2 The results of the extracted parameter for samples with low LB, LD, CB, and CD properties.

Case	The input values	Error bars of α , β , θ_d , D , γ , and R , respectively
Low LB	($\alpha = 3$ -deg, $\beta = 3$ -deg, $\theta_d = 35$ -deg, $D = 0.4$, $\gamma = 15$ -deg, and $R = 0.1$)	± 0.366 -deg, ± 0.04 -deg, ± 0.176 -deg, ± 0.003 , ± 0.012 -deg, and ± 0.001
Low LD	($\alpha = 50$ -deg, $\beta = 60$ -deg, $\theta_d = 35$ -deg, $D = 0.05$, $\gamma = 15$ -deg, and $R = 0.1$)	± 0.018 -deg, ± 0.033 -deg, ± 1.472 -deg, ± 0.003 , ± 0.01 -deg, and ± 0.002
Low CB	($\alpha = 50$ -deg, $\beta = 60$ -deg, $\theta_d = 35$ -deg, $D = 0.4$, $\gamma = 0.1$ -deg, and $R = 0.1$)	± 0.028 -deg, ± 0.032 -deg, ± 0.185 -deg, ± 0.003 , ± 0.027 -deg, and ± 0.001
Low CD	($\alpha = 50$ -deg, $\beta = 60$ -deg, $\theta_d = 35$ -deg, $D = 0.4$, $\gamma = 15$ -deg, and $R = 0.01$)	± 0.028 -deg, ± 0.032 -deg, ± 0.185 -deg, ± 0.003 , ± 0.027 -deg, and ± 0.001

In deriving the theoretical values of the output Stokes parameters, the effective properties of the optical sample were assigned as follows: $\alpha = 50$ -deg, $\beta = 60$ -deg, $\theta_d = 35$ -deg, $D = 0.4$, $\gamma = 15$ -deg, and $R = 0.1$. The values of α , β , θ_d , D , γ , and R were then extracted from the perturbed values of the output Stokes parameters using Eqs. (24), (26), (27), (16), (17), and (20), respectively. From inspection, the error bars of parameters α , β , θ_d , D , γ , and R have values of just ± 0.022 -deg, ± 0.038 -deg, ± 0.174 -deg, ± 0.005 , ± 0.066 -deg, and ± 0.003 , respectively. Thus, it is inferred that the analytical model is robust toward experimental errors in the output Stokes parameters.

3.3 Resolution of Extracted Parameter Values for Samples with Low LB, LD, CB, and CD Properties

For samples with close to zero retardance ($\beta \approx 0$), the Mueller matrix of linear birefringence (Eq. 1) is a unit matrix for any value of the orientation angle of LB ($\alpha = 0$ -deg to 180 -deg). In other words, for a sample with $\beta \approx 0$, the values obtained

for the orientation angle of LB from Eq. (24) are unreliable. Similarly, for samples with a linear dichroism close to zero ($D \approx 0$), the Mueller matrix of linear dichroism [Eq. (2)] is a unit matrix for any value of the linear dichroism axis angle ($\theta_d = 0$ -deg to 180 -deg). In other words, the results obtained for θ_d from Eq. (16) are unreliable. Therefore, the performance of the proposed analytical model in extracting the optical parameters of samples with a low LB, low LD, low CB, and low CD are evaluated as shown in Table 2.

The extracted values of the sample parameters are compared with the input values given assumed errors of ± 0.005 in the values of the output Stokes parameters. Significantly, the results presented in Table 2 show that even though the orientation angle of LB is highly sensitive to errors in the output Stokes parameters, the extracted values of the CB, LD, and CD properties deviate only slightly from the input values. In other words, the decoupled nature of the analytical model prevents the error in the orientation angle of LB from contaminating the extracted values of the remaining parameters, and improves their precision as a result. Similarly, in low LD case, the extracted values of the

Table 3 The comparison between nondepolarizing method and depolarizing method with low depolarization case.

Parameters	Input value (Case #1)		
	Input control values	Estimated values of (Ghosh et al. ²²)	Extracted values (the proposed study)
Orientation angle of LB (α)	X	X	92.4-deg
Linear birefringence (β)	0.83 (rad)	0.79 (rad)	0.88 (rad)
Optical rotation (γ)	2.14-deg	2.05-deg	2.06-deg
Orientation angle of LD (θ_d)	X	X	4.45-deg
Linear dichroism (D)	0	0.02 (diattenuation)	0.018
Circular dichroism (R)	0	X	0.002
Depolarization coefficient	0.19	0.21	X

^aNote: the notation X in the tables indicates none value.

Table 4 The comparison between nondepolarizing method and depolarizing method with high depolarization case.

Parameters	Estimated values of (Ghosh et al. ²³)	Extracted values (the proposed study)
Orientation angle of LB (α)	88.9-deg	89.11-deg
Linear birefringence (β)	0.905 (rad)	1.3 (rad)
Optical rotation (γ)	2.09-deg	2.3-deg
Orientation angle of LD (θ_d)	X	93.24-deg
Linear dichroism (D)	0.019 (diattenuation)	0.016
Circular dichroism (R)	X	0.004
Depolarization coefficient	0.798	X

^aNote: the notation X in the table indicates none value.

LB, CB, and CD properties deviate only slightly from the input values despite the error in the extracted value of θ_d . Overall, the ability of the proposed method to extract the orientation angle of LB of samples with a low degree of birefringence can be reliable when retardance is larger than 3-deg. Moreover, the values of orientation angle of LD can be reliable when linear dichroism is larger than 0.05. The ability of the proposed method to extract the optical parameters of samples with CB larger than 0.1-deg or CD larger than 0.01 are reliable with the input Stokes parameters given assumed errors of ± 0.005 .

4 Comparison Between the Proposed Nondepolarizing Method and Depolarizing Method

To compare the results by the proposed nondepolarizing Mueller matrix method and depolarizing Mueller matrix method, one demonstration was established by using the results of Mueller matrix in Ghosh et al.²² In Table 3, the Mueller matrix was experimentally recorded in the forward scattering geometry from the polyacrylamide phantom having degree of strain-induced birefringence (extension = 2 mm applied along the vertical direction), chiral (concentration of sucrose = 1 M corresponding to magnitude of optical activity = 1.96 deg cm⁻¹), turbid (scattering coefficient = 3 mm⁻¹, value for anisotropy parameter of particles in polyacrylamide calculated from Mie theory = 0.95).²² All elements of the Mueller matrix was inserted into Eqs. (24), (26), (27), (16), (17), and (20) in order to extract the values of α , β , γ , θ_d , D , and R , respectively. In Table 3, the results show that with depolarization coefficient equal to 0.19 (low depolarization), the extracted parameters by the proposed method are equivalent to those by the method in Ghosh et al.²²

Another comparison was established by using the results of Mueller matrix in Ghosh et al.²³ with high depolarization (i.e. depolarization coefficient equal to 0.798). The Monte Carlo-generated Mueller matrix and the decomposed matrices for a birefringent, chiral, turbid medium (anisotropy in

refractive index = 1.36×10^{-5} , which corresponds to a value of linear retardance = 1.35 rad for a path length of 10 mm, optical activity = 1.96 deg cm⁻¹, scattering coefficient = 6 mm⁻¹, and average cosine of scattering angle = 0.935) are introduced in Ghosh et al.²³ The axis of linear birefringence was kept along the vertical (Y) direction (orientation angle of LB = 90-deg) in the simulation. Table 4 compares the values of α , β , γ , θ_d , D , and R obtained from Ghosh et al.²³ and the proposed study. It is observed that a good agreement exists between the extracted values of LD/CD (i.e., θ_d , D , and R) by the proposed method and those by the method in Ghosh et al.²³ with high depolarization. It is explained that the first element of the depolarization Mueller matrix equals one and other elements (except diagonal) are closed to zero.^{20-23,27,34,35} Thus, the first row of effective Mueller matrix [M_{RD}] (i.e. m_{11} , m_{12} , m_{13} , and m_{14}) in Eq. (23) does not change when the depolarization Mueller matrix is multiplied in front of the effective Mueller matrix. In other words, Eqs. (16), (17), and (20) also can be used to extract the values of θ_d , D , and R in the case of the depolarizing Mueller matrix.

Interestingly, the extracted values of LB/CB (i.e., α , β , and γ) are also closed to the corresponding input values (i.e., orientation angle of LB [α] 90-deg and value of linear retardance [β] 1.35 rad in the simulation). With a separate series of comparisons, it is found that when the difference between the two linear depolarization values and circular depolarization value are small (see the depolarization Mueller matrix in Ghosh et al.²³), the extracted values of LB/CB are still reliable in high depolarization case.

5 Influence of the Order of [M_R] and [M_D]

Researchers have proved that for the depolarizing Mueller matrix, the decomposition in [M_Δ][M_R][M_D] is a natural generalization of the polar decomposition.^{27,34,35,39,40} Thus, for the nondepolarizing Mueller matrix, the decomposition in [M_R][M_D] is generally used for the decomposition. The decomposition in [M_Δ][M_R][M_D] clearly separates the depolarizing component ([M_Δ]) from the nondepolarizing component ([M_R][M_D]).²⁷

Table 5 Influence of order in Mueller matrix using GA and the proposed study.

Input value			
$M_1 = \begin{pmatrix} 0.7769 & -0.1142 & 0.1979 & 0.1538 \\ 0.0603 & 0.5392 & 0.1998 & 0.4480 \\ 0.2679 & -0.4327 & 0.5652 & 0.2783 \\ 0.0214 & -0.2506 & -0.4556 & 0.5077 \end{pmatrix} \text{ (Case \#1)}$			
$M_2 = \begin{pmatrix} 0.7429 & 0.1371 & 0.2375 & 0.2857 \\ 0.3905 & 0.1669 & 0.4207 & 0.5853 \\ -0.0049 & -0.3233 & 0.4758 & -0.2531 \\ -0.0662 & -0.5304 & -0.2190 & 0.2646 \end{pmatrix} \text{ (Case \#2)}$			
Parameters	Estimated values ([M_R][M_D]) using GA	Estimated values ([M_D][M_R]) using GA	Estimated values (the proposed study)
Case #1			
Orientation angle of LB (α_S)	$\alpha_S = 59.999$ -deg	$\alpha_S = 60.954$ -deg	$\alpha_S = 59.997$ -deg
Linear birefringence (β_S)	$\beta_S = 44.999$ -deg	$\beta_S = 45.683$ -deg	$\beta_S = 45.001$ -deg
Optical rotation (γ_S)	$\gamma_S = 15.001$ -deg	$\gamma_S = 14.637$ -deg	$\gamma_S = 15.000$ -deg
Orientation angle of LD (θ_{dS})	$\theta_{dS} = 59.998$ -deg	$\theta_{dS} = 38.657$ -deg	$\theta_{dS} = 59.994$ -deg
Linear dichroism (D_S)	$D_S = 0.3$	$D_S = 0.353$	$D_S = 0.3$
Circular dichroism (R_S)	$R_S = 0.1$	$R_S = 0.015$	$R_S = 0.1$
Note: Subscript "s" indicates "sample"	($E_\varphi = 2.04 \times 10^{-8}$)	($E_\varphi = 2.06 \times 10^{-8}$)	Note: Input Mueller matrix of [M] into Eqs. (24), (26), (27), (16), (17) and (20)
Case #2			
Orientation angle of LB (α_S)	$\alpha_S = 29.999$ -deg	$\alpha_S = 31.114$ -deg	$\alpha_S = 30.001$ -deg
Linear birefringence (β_S)	$\beta_S = 60.002$ -deg	$\beta_S = 62.237$ -deg	$\beta_S = 60.008$ -deg
Optical rotation (γ_S)	$\gamma_S = 24.999$ -deg	$\gamma_S = 24.415$ -deg	$\gamma_S = 24.998$ -deg
Orientation angle of LD (θ_{dS})	$\theta_{dS} = 30.001$ -deg	$\theta_{dS} = 0.236$ -deg	$\theta_{dS} = 30.001$ -deg
Linear dichroism (D_S)	$D_S = 0.4$	$D_S = 0.522$	$D_S = 0.4$
Circular dichroism (R_S)	$R_S = 0.2$	$R_S = 0.001$	$R_S = 0.2$
	($E_\varphi = 3.8 \times 10^{-8}$)	($E_\varphi = 0.016$)	

For completely polarized incident light, the decrease of the polarization degree is solely caused by the depolarizing component. Thus, [M_Δ][M_R][M_D] is useful to have the depolarizing component following the nondepolarizing component for the interpretation of experimental data. Also, Morio and Goudail³⁴ showed that the decomposition proposed by Lu and Chipman always leads to physical Mueller matrices.

Since Mueller matrices do not commute, the influence of the order in nondepolarizing Mueller matrices is investigated in this section. The influence of the order of nondepolarizing Mueller matrices for extracting the six effective optical parameters is verified using genetic algorithms (GAs). Thereafter, simulations are performed to compare the two set of results obtained from product of [M_R][M_D] and [M_D][M_R] using GAs with the extracted results using the proposed method.

The GAs provide a powerful technique for computing the exact or approximate solutions to a wide variety of optimization and classification type problems.^{41,42} In the present study, the candidate solution strings contain six elements corresponding to α_S , β_S , γ_S , θ_S , D_S , and R_S . In generating the candidate solutions, the search spaces for α_S , β_S , γ_S , θ_S , D_S , and R_S were specified as $0\text{-deg} \leq \alpha_S \leq 180\text{-deg}$, $0\text{-deg} \leq \beta_S \leq 360\text{-deg}$, $0\text{-deg} \leq \gamma_S \leq 180\text{-deg}$, $0\text{-deg} \leq \theta_S \leq 180\text{-deg}$, $0 \leq D_S \leq 1$, and $-1 \leq R_S \leq 1$, respectively. The quality of each candidate solution is evaluated using a fitness function based on the distance between the elements of the input Mueller matrix and the elements of the product of [M_R][M_D] or [M_D][M_R], respectively. In other words, the error function has the form:

$$E_\varphi = \sum_{i=1}^{16} (\varphi_{i,[M_{\text{Input}}]} - \varphi_{i,[M_R][M_D]})^2 \quad (39)$$

or

$$E_{\varphi} = \sum_{i=1}^{16} (\varphi_{i,[M_{\text{Input}}]} - \varphi_{i,[M_D][M_R]})^2 \quad (40)$$

where $\varphi_{i,[M_{\text{Input}}]}$ represents the elements of the input Mueller matrix and $\varphi_{i,[M_R][M_D]}$ and $\varphi_{i,[M_D][M_R]}$ represent the corresponding elements of $[M_R][M_D]$ and $[M_D][M_R]$. In other words, the objective of the GA is to determine the values of $\alpha_S, \beta_S, \gamma_S, \theta_S, D_S,$ and R_S , which minimize the error function.

Table 5 compares the extracted values of $\alpha_S, \beta_S, \gamma_S, \theta_S, D_S,$ and R_S obtained from the GA ($[M_R][M_D]$ and $[M_D][M_R]$) and from the proposed study method. With a separate series of simulations, it is observed that a good agreement exists between the extracted values in $[M_R][M_D]$ and the proposed study method. In the $[M_D][M_R]$ case, only the extracted values of $\alpha_S, \beta_S,$ and γ_S are equivalent to the extracted values of two cases. Thus, the order of $[M_R]$ and $[M_D]$ affected the effective parameters of anisotropic optical materials in LD/CD, but not in LB/CB properties.

6 Experimental Verification of Proposed Analytical Model

6.1 Experimental Setup

Figure 2 presents a schematic illustration of the experimental setup used to verify the performance of the proposed analytical model. In performing the experiments, the input light was provided by a frequency-stable He-Ne laser (SL 02/2, SIOS Co.) with a central wavelength of 632.8 nm. In addition, a polarizer (GTH5M, Thorlabs Co.) and quarter-wave plate (QWP0-633-04-4-R10, CVI Co.) were used to produce four linear polarization lights (0-deg, 45-deg, 90-deg and 135-deg) and two circular polarization lights (right-handed and left-handed). A neutral density filter (NDC-100-2, ONSET Co.) and power meter detector (8842A, OPHIT Co.) were used to ensure that each of the input polarization lights had an identical intensity. Note that for samples with no linear dichroism, the output Stokes parameters can be normalized as S_C/S_0 since the terms m_{12}, m_{13} and m_{14} in Eq. (5) are non-zero. Thus, there is no need to ensure that the six input lights have an identical optical intensity before entering the sample. However, for samples with linear dichroism, the output Stokes parameters cannot be normalized in this way, and thus the neutral density filter and power meter detector are required.

The output Stokes parameters were computed from the intensity measurements obtained using a commercial Stokes polarimeter (PAX5710, Thorlabs Co.) at a sampling rate of 30 samples per second. A minimum of 1024 data points were obtained for the effective parameters ($\alpha, \beta, \theta_d, D, \gamma,$ and R) of each sample. Of these data points, 100 points were then chosen in order to calculate the mean value of each parameter.

The validity of the proposed measurement method was evaluated using different optical samples, namely a quarter-wave plate (QWP0-633-04-4-R10, CVI Co.), a half-wave plate (QWP0-633-04-2-R10, CVI Co.), the de-ionized water with containing D-glucose, a polarizer (GTH5M, Thorlabs Co.), a polarization controller, and a polymer polarizer (LLC2-82-18S, OPTIMAX Co.) baked in an oven at 150 °C for 100 min.

Also, a composite sample comprising a quarter-wave plate, a half-wave plate and a polarizer in aligned or non-aligned principal axis were tested. Note that the polarization controller was

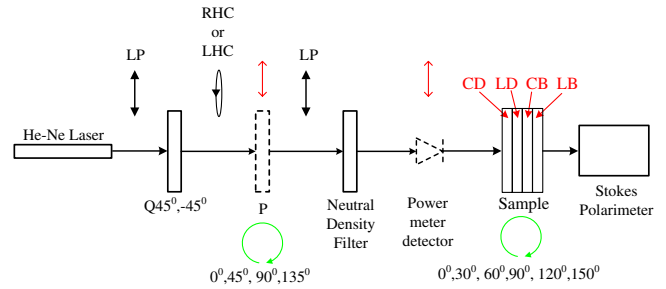


Fig. 2 Schematic illustration of experimental measurement system.

used to evaluate the performance of the proposed method in extracting the parameters of samples with circular dichroism only. Meanwhile, the baked polarizer was chosen in order to evaluate the performance of the proposed method in measuring the optical parameters of samples with both linear birefringence and linear dichroism.

6.2 Experimental Results

6.2.1 Quarter-wave plate (LB property only)

Figure 3 illustrates the experimental results obtained for the effective properties of the quarter-wave plate (QW). From inspection, the standard deviations of the orientation angle and phase retardance measurements are found to be just 0.04-deg and 0.013-deg, respectively. In other words, the ability of the proposed method to extract the properties of samples with linear birefringence only is confirmed. As expected, the linear dichroism, optical rotation angle and circular dichroism parameters have a value close to zero at all values of the orientation angle. As discussed in Sec. 3.3, the proposed analytical model yields reliable results for the orientation angle of LD only for samples with a linear dichroism greater than or equal to 0.05. In the present sample, the linear dichroism is close to zero, and thus the orientation angle of LD varies randomly in the range of 0-deg to 180-deg as the orientation angle of LB is increased [see Fig. 3(b)]. As expected, Figs. 3(c) and 3(d) show that the optical rotation angles and values of circular dichroism of the quarter-wave plate are also close to zero.

6.2.2 Half-wave plate and de-ionized water containing D-glucose (CB property only)

Half-wave plate (CB property only). In general, the elements in the Mueller matrix for an optically active material are different from those in the Mueller matrix for a half-wave plate. The Mueller matrix of a half-wave plate with an optical rotation γ_H has the form as

$$M_{HP} = \begin{bmatrix} 1 & 0 & 0 & 0 \\ 0 & \cos(4\gamma_H) & \sin(4\gamma_H) & 0 \\ 0 & \sin(4\gamma_H) & -\cos(4\gamma_H) & 0 \\ 0 & 0 & 0 & -1 \end{bmatrix}. \quad (41)$$

Thus, in computing the optical rotation angle of the half-wave plate, the formula of linear retardance (β) is revised as:

$$\beta = \tan^{-1} \left(\frac{A_{34}}{\cos(2\alpha)A_{44}} \right), \quad (42)$$

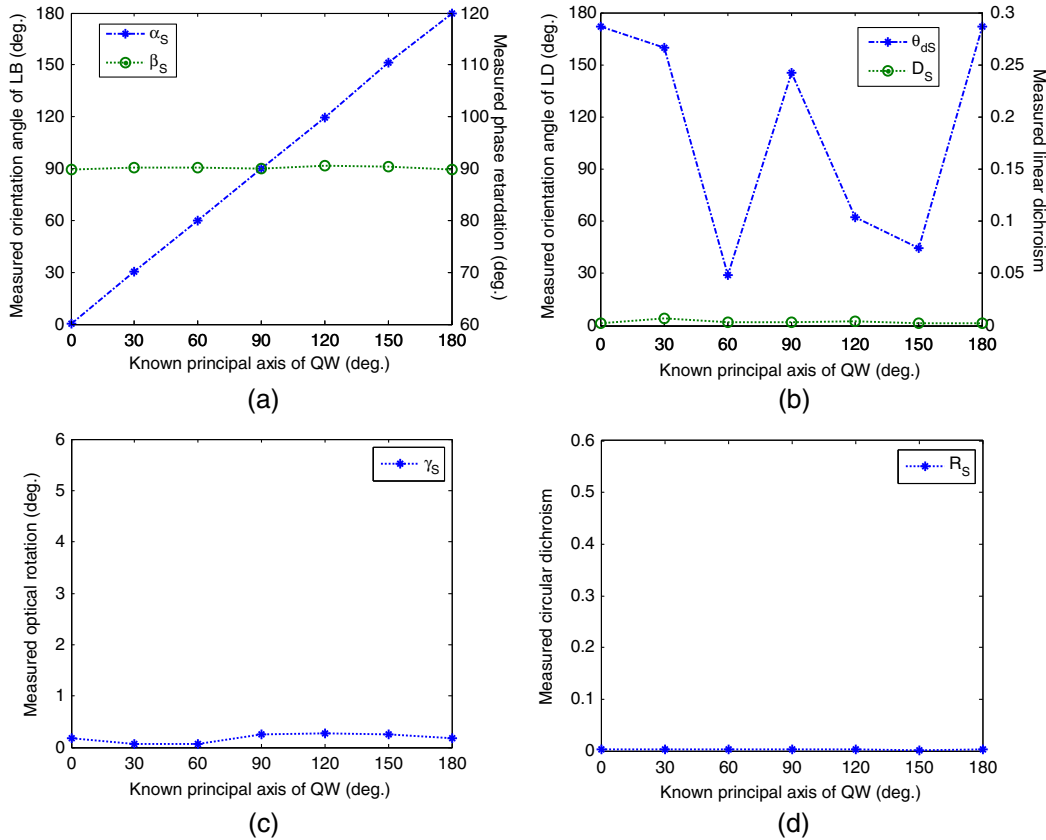


Fig. 3 Experimental results for effective parameters of quarter-wave plate (QW).

or

$$\beta = \cos^{-1}(-A_{44}). \quad (43)$$

Then, the formula of optical rotation (γ) is revised as:

$$\gamma = \frac{1}{2} \tan^{-1} \left(\frac{A_{23} + A_{32}}{A_{22} - A_{33}} \right), \quad (44)$$

or

$$\gamma = \frac{1}{2} \tan^{-1} \left(\frac{C_2 A_{22} + C_1 A_{23}}{C_1 A_{22} - C_2 A_{23}} \right). \quad (45)$$

Figure 4 presents the experimental results for the effective properties of the half-wave plate. Figure 4(c) shows that a good agreement is obtained between the measured value of the optical rotation angle and the actual value of the optical rotation angle over the considered range of 0-deg to 90-deg. From inspection, the standard deviation of the optical rotation angle is found to be just 0.008-deg. As discussed in Sec. 3.3, the analytical model yields reliable results for the orientation angle of LB only for samples with a phase retardance greater than or equal to 3-deg. Similarly, reliable results for the orientation angle of LD are obtained only for samples with a linear dichroism greater than or equal to 0.05. Figures 4(a) and 4(b) show that both the retardance and the linear dichroism of the half-wave plate are close to zero. Thus, the extracted values of the orientation angle of LB and orientation angle of LD vary randomly as the optical rotation angle is increased. As expected, Fig. 4(d) shows that the circular dichroism of the half-wave plate is also close to zero.

De-ionized water containing D-glucose (CB property only). Figure 5 illustrates the experimental results obtained for the effective parameters of the de-ionized water with containing D-glucose (Merck Ltd.). The D-glucose was poured into a container of de-ionized water. The average measured values of the optical parameters of the sample with different concentration of glucose from 0 to 1 M in increments of 0.1 M are summarized. The container is glass and its width is 12.5 mm outside and 10 mm inside. Distance from center of sample to surface of detector is 23 mm. Figure 5(c) shows the measured value of the optical rotation angle regarding to the concentration of glucose over the considered range of 0 to 1 M. The sensitivity of the D-glucose measurement is estimated 1.9 M/l, and it is a good agreement with Lo and Yu.⁴³ From inspection, the standard deviation of the optical rotation angle is found to be just 0.01-deg. As discussed in Sec. 3.3, the analytical model yields reliable results for the orientation angle of LB only for samples with a phase retardance greater than or equal to 3-deg. Similarly, reliable results for the orientation angle of LD are obtained only for samples with a linear dichroism greater than or equal to 0.05. Figures 5(a) and 5(b) show that both the retardance and the linear dichroism of the de-ionized water with containing D-glucose are close to zero. Thus, the extracted values of the orientation angle of LB and orientation angle of LD vary randomly as the concentration of glucose is increased. As expected, Fig. 5(d) shows that the circular dichroism of the de-ionized water with containing D-glucose is also close to zero.

6.2.3 Polarizer (LD property only)

Figure 6 presents the experimental results for the effective parameters of the polarizer. As expected, the linear dichroism

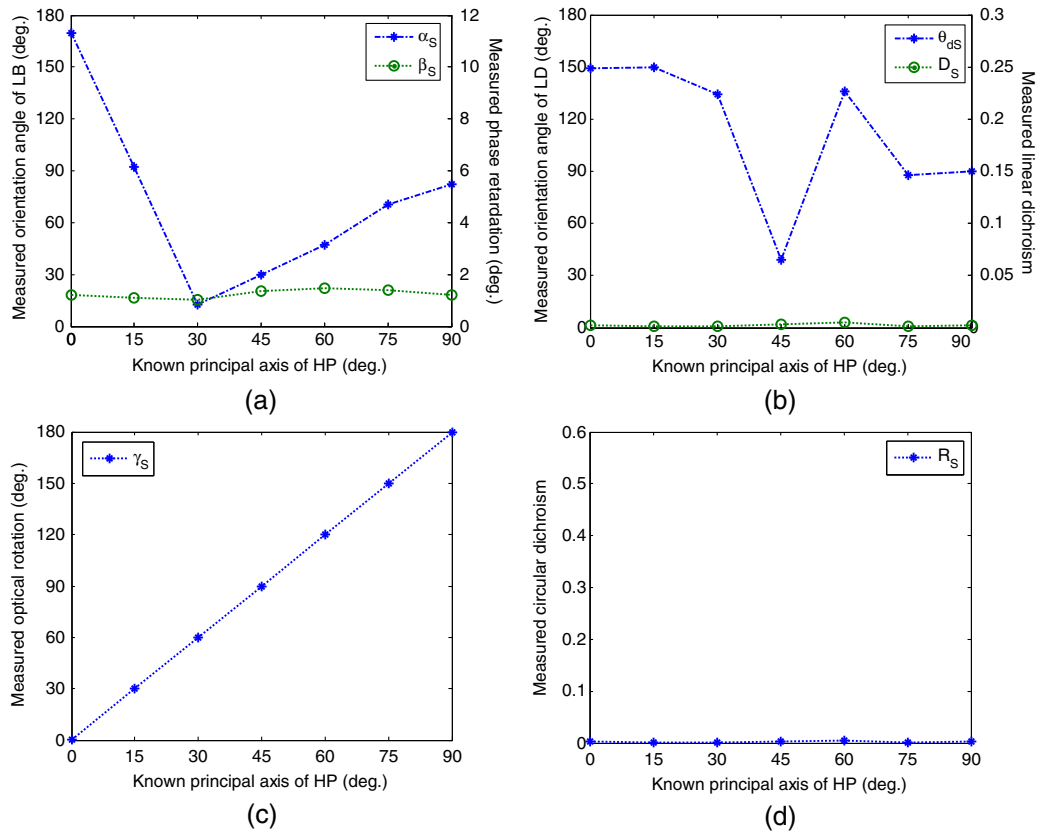


Fig. 4 Experimental results for effective parameters of half-wave plate (HP).

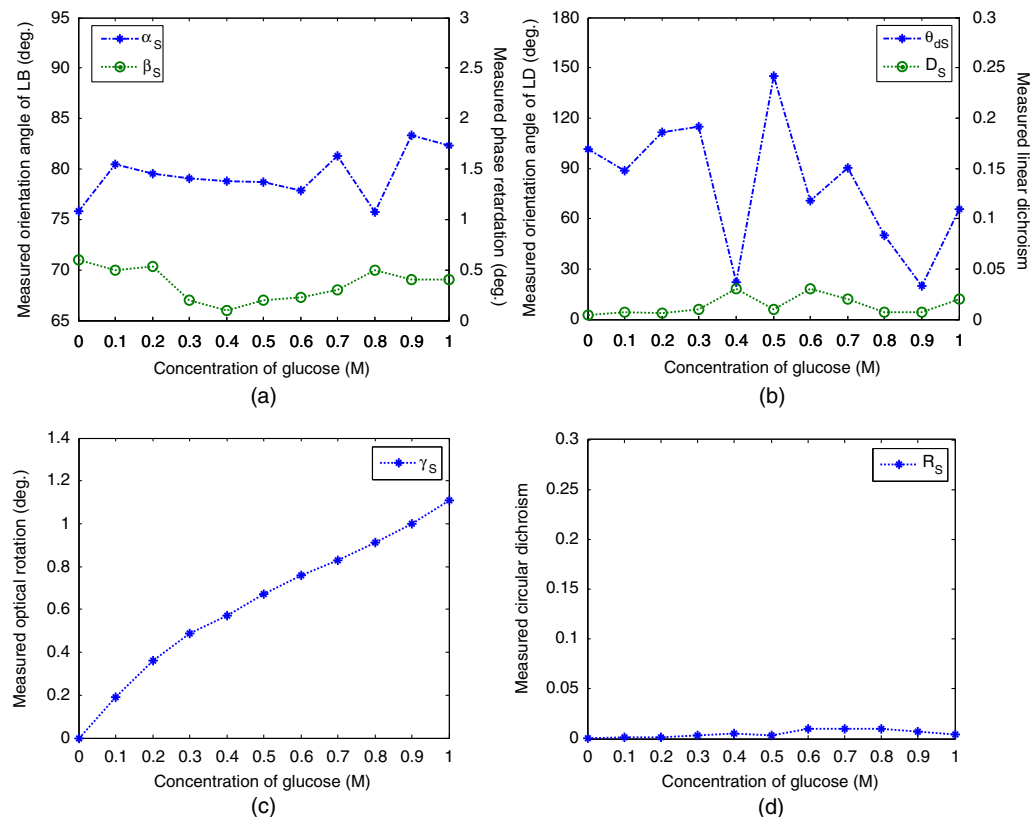


Fig. 5 Experimental results for effective parameters of de-ionized water with containing D-glucose.

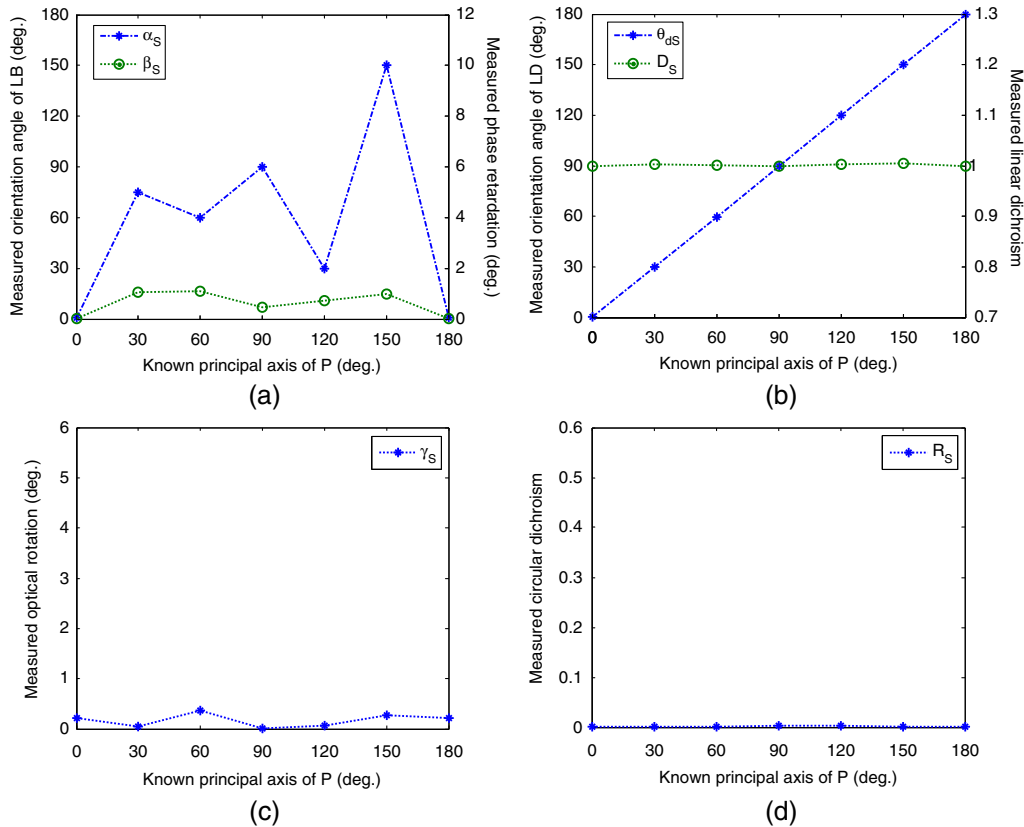


Fig. 6 Experimental results for effective parameters of polarizer (P).

has a value close to one [see Fig. 6(b)]. Moreover, a good agreement is observed between the measured values of the orientation angle of LD and the known values. From inspection, the standard deviations of θ_d and D are found to be just 0.007-deg and 1.42×10^{-4} , respectively. In other words, the ability of the proposed analytical model to extract the parameters of samples with pure LD properties is confirmed. Figures 6(c) and 6(d) confirm that the CB and CD properties of the polarizer are close to zero. As discussed in Sec. 3.3, reliable results are obtained for the orientation angle of LB provided that the phase retardance has a value greater than or equal to 3-deg. As shown in Fig. 6(a), the polarizer has a retardance of less than 2-deg. Thus, the extracted value of the orientation angle of LB varies randomly in the range of 0 to 180-deg as the orientation angle of LD is increased. Note that in previous studies by the current group,^{32,33} both the retardance and the orientation angle of LB of the polarizer were found to vary randomly with the orientation angle of LD. However, in the present study, the extracted value of the retardance is approximately constant. In other words, the decoupled nature of the analytical model proposed in this study successfully resolves the “multiple solutions” problem found in Chen et al.³² and Lo et al.³³ for samples with a linear dichroism of $D = 1$.

6.2.4 Polarization controller (CD property only)

In the present study, a sample with pure CD properties was simulated using a polarization controller comprising a half-wave plate sandwiched between two quarter-wave plates and a neutral density filter (NDF). In performing the measurement process, the experimental settings of the polarization controller

and NDF required to replicate a pure CD sample were determined using the genetic algorithm (GA) method described in Refs. 41, 42. That is, having specified the desired value of the circular dichroism (e.g., $R = 0.2$), the orientation angle of the two quarter-wave plates (α_1 and α_2), the optical rotation angle of the half-wave plate (γ_1), and the output intensity of the NDF were tuned in accordance with the results obtained from the GA such that the following condition was satisfied for each of the six input polarization lights.

$$S_c = [M_{QW1}][M_{HP}][M_{QW2}][M_{NDF}]\hat{S}_c \approx [M_{cd}]\hat{S}_c \quad (46)$$

where S_c are the output Stokes parameters obtained when using the simulated CD sample, $[M_{QW1}]$ and $[M_{QW2}]$ are the Mueller matrices of the two quarter-wave plates, $[M_{HP}]$ is the Mueller matrix of the half-wave plate, $[M_{NDF}]$ is the Mueller matrix of the neutral density filter, and $[M_{cd}]$ is the theoretical Mueller matrix of a sample with CD properties only. Six different values of α_1 , α_2 , γ_1 , and the NDF output intensity were obtained for input lights of $S_{0\text{-deg}}$, $S_{45\text{-deg}}$, $S_{90\text{-deg}}$, $S_{135\text{-deg}}$, S_{RHC} , and S_{LHC} , respectively. In performing the experiments, the polarization controller and NDF were set accordingly, and the resulting output Stokes parameters were measured using a commercial polarimeter (PAX5710, Thorlabs Co.). The circular dichroism of the simulated sample was then calculated using Eq. (20) in Sec. 2.

Figure 7(d) shows that a good agreement is obtained between the measured values of the circular dichroism and the simulated values. From inspection, the standard deviation of the measured values is just 2.94×10^{-4} . Thus, the ability of the proposed

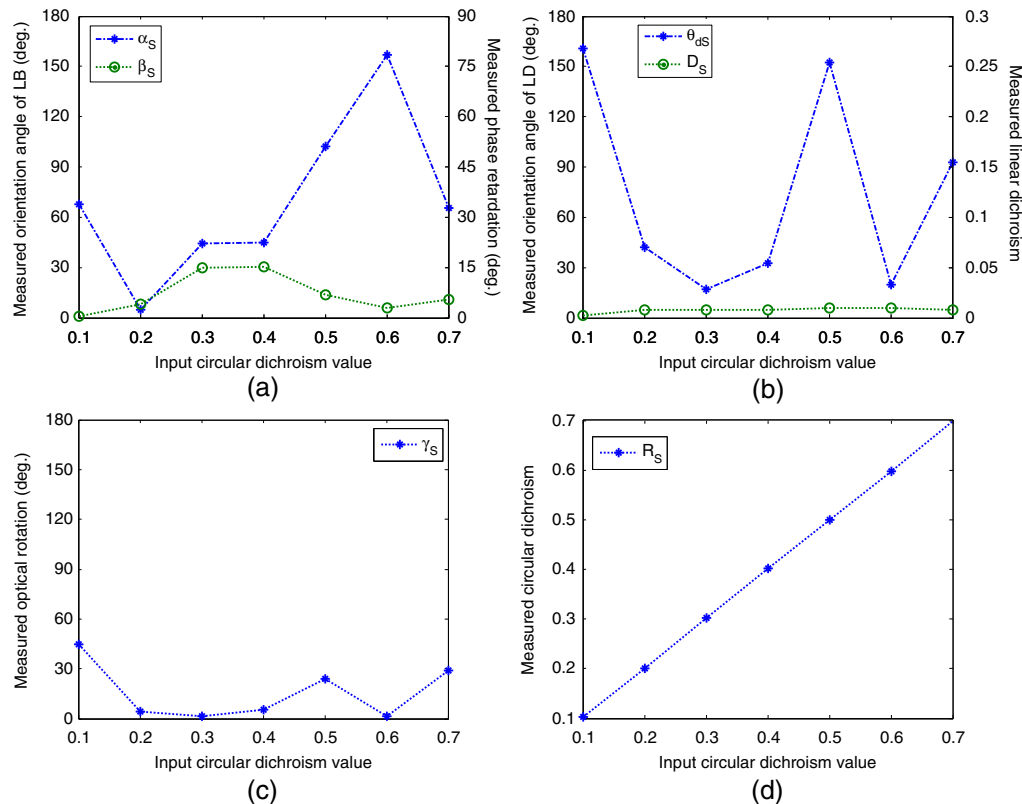


Fig. 7 Experimental results obtained for effective parameters of simulated CD sample.

method to extract the parameters of an optical sample with CD properties only is confirmed. As expected, Fig. 7(b) shows that the linear dichroism of simulated sample is close to zero. Thus, the extracted values of the orientation angle of LD vary randomly as the simulated circular dichroism value is increased. Note that for a sample with pure CD properties, the phase retardance and optical rotation angle are very small (zero, ideally). However, the polarization controller and NDF do not provide sufficient parameters for the actual LB and CB properties of the simulated sample to be explored. As shown in Figs. 7(a) and 7(c), the extracted value of the orientation angle and the linear retardance of LB and the optical rotation of CB varies randomly in the range of 0 to 180-deg as the simulated circular dichroism value is increased.

6.2.5 Baked polarizer (LB and LD properties)

Figure 8 illustrates the experimental results obtained for the LB and LD properties of the baked polarizer (BP). As expected, the measured values of the optical rotation angle and circular dichroism are close to zero [see Figs. 8(c) and 8(d)]. Due to the prolonged exposure of the polarizer to a high-temperature environment, the input light leaks through one of the LD axes. Thus, as shown in Fig. 8(b), the linear dichroism has a value close to 1. Moreover, it can be seen that a good agreement exists between the measured values of the orientation angle of LD and the given values. The average value of the phase retardance is found to be 16.92-deg [see Fig. 8(a)]. In addition, a good correlation is observed between the measured values of the orientation angle of LB and the given values. From inspection, the standard deviations of the extracted values of α , β , θ_d , and D are found to be just 0.03-deg, 0.03-deg, 0.01-deg and

4.16×10^{-4} , respectively. In other words, the proposed analytical model enables the parameters of hybrid samples with both LB and LD properties to be accurately determined.

6.2.6 Composite sample comprising quarter-wave plate, half-wave plate, and polarizer (LB, CB, and LD properties)

Aligned principal axis of quarter-wave plate, half-wave plate and polarizer. Figure 9 shows the experimental results obtained for a composite sample comprising a polarizer (LD), a half-wave plate (CB) and a quarter-wave plate (LB). As shown in Figs. 9(a)–9(c), a good agreement is obtained between the measured values and the known values of the orientation angle of LB, orientation angle of LD, and optical rotation, respectively. Moreover, as expected, the quarter-wave plate has a phase retardance of approximately $\beta = 90$ -deg, the polarizer has a linear dichroism of approximately $D \approx 1$. As expected, the measured values of the circular dichroism are close to zero [see Fig. 9(d)]. Thus, the ability of the proposed measurement method to extract the effective parameters of samples with both linear/circular birefringence and linear dichroism is confirmed.

Non-aligned principal axis of quarter-wave plate, half-wave plate, and polarizer. Figure 10 illustrates the experimental results obtained for the effective properties of a composite sample comprising a polarizer (LD), a half-wave plate (CB) and a quarter-wave plate (LB) in non-aligned principal axis angle. It is noted that the average measured values of the effective parameters of the composite sample with different principal axis angle of quarter-wave plate from 0 to 90-deg in increments of 15-deg whereas the principal axis angle of polarizer fixed to

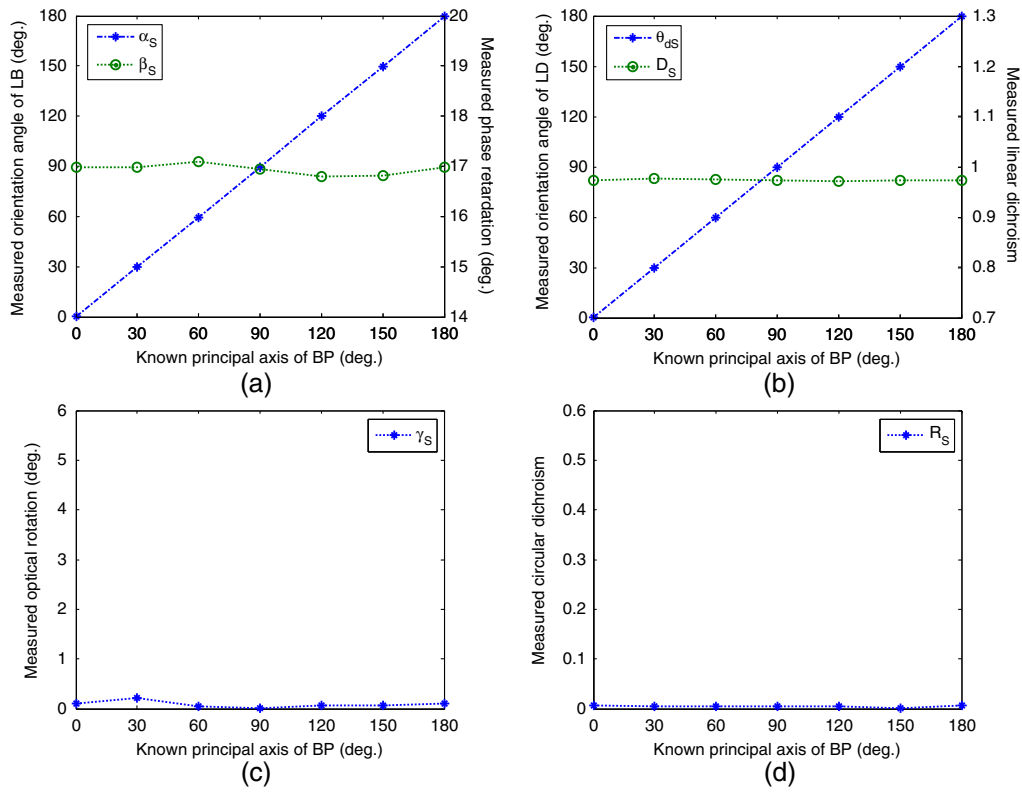


Fig. 8 Experimental results obtained for effective parameters of baked polarizer (BP).

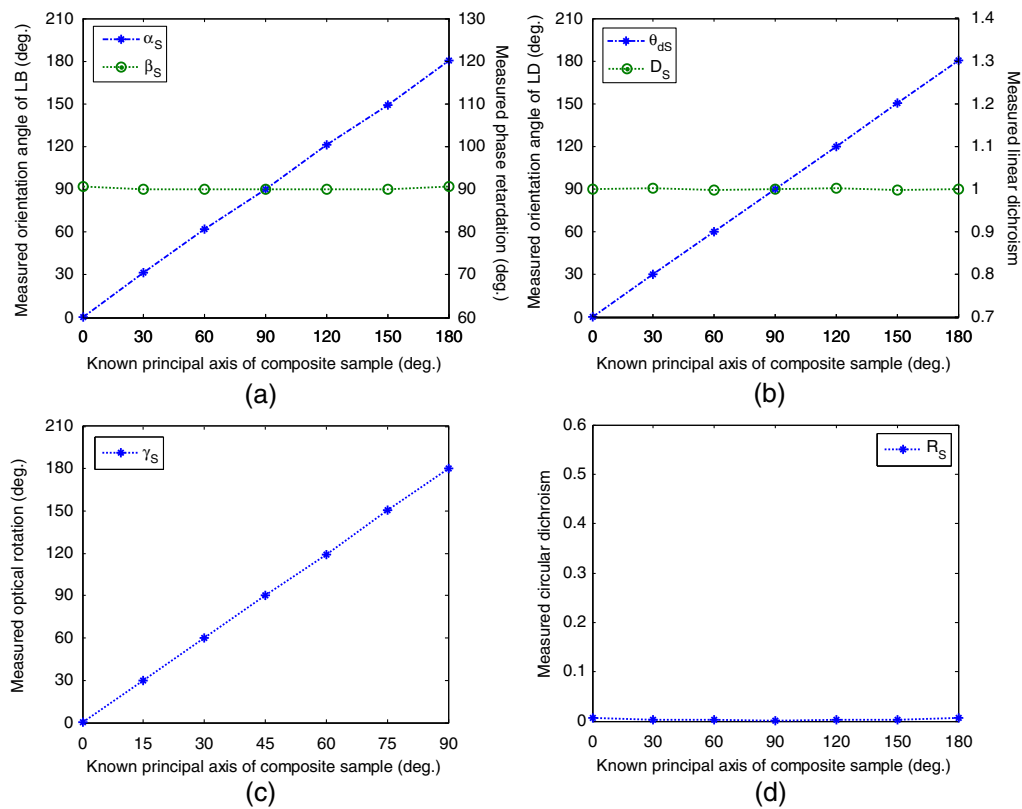


Fig. 9 Experimental results for effective parameters of composite sample with aligned principal axis.

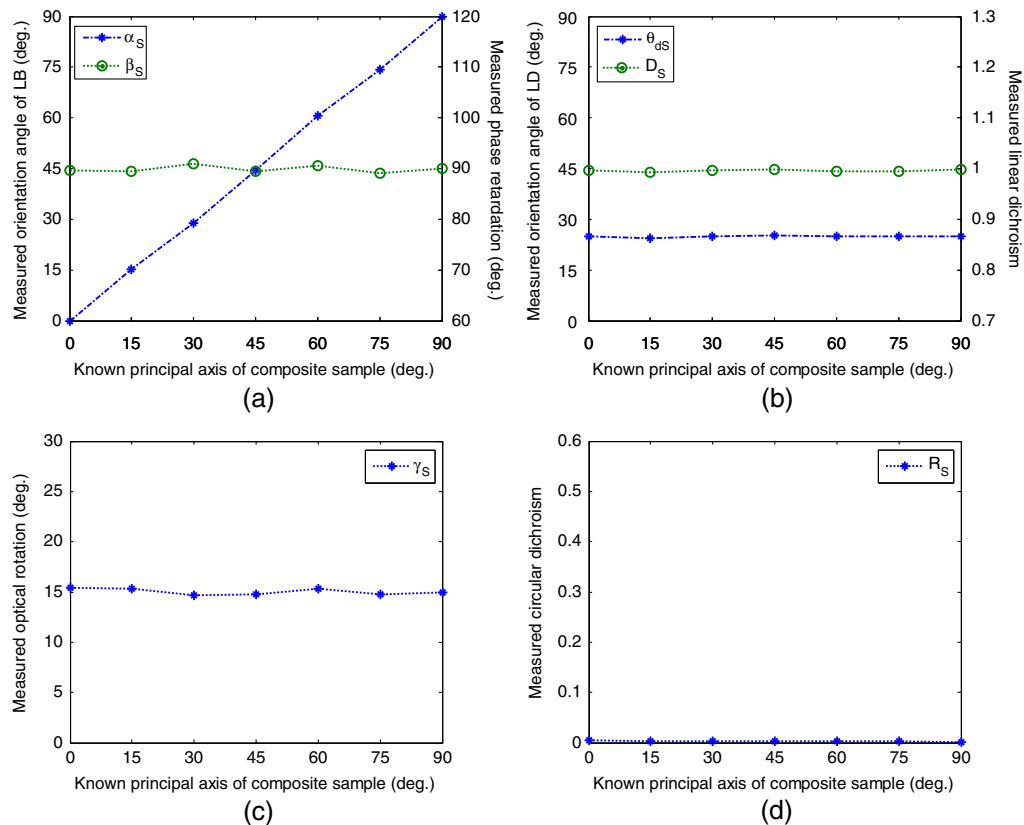


Fig. 10 Experimental results for effective parameters of composite sample with non-aligned principal axis.

25-deg and the principal axis angle of half-wave plate fixed to 15-deg are summarized.

As shown in Figs. 10(a)–10(c), a good agreement is obtained between the measured values and the known values of the orientation angle of LB, orientation angle of LD, and optical rotation, respectively. Moreover, as expected, the quarter-wave plate has a phase retardance of approximately $\beta = 90$ -deg, the polarizer has a linear dichroism of approximately $D \approx 1$. As expected, the measured values of the circular dichroism are close to zero [Fig. 10(d)]. Once again, the ability of the proposed measurement method to extract the effective parameters of samples with LB, CB, and LD in non-aligned principal axis angle is confirmed.

In summary, the experimental results confirm that the decoupled nature of the analytical model improves accuracy and the ability to extract the parameters of optical samples with only linear birefringence, circular birefringence, linear dichroism, or circular dichroism property without using compensation technique or pretreatment. Moreover, the unreliable result of one effective parameter problem inherent in others is avoided [see Eqs. (24), (26), (27), (16), (17), and (20)]. Furthermore, the “multiple solutions” problem when extracting the LB properties of a sample with a linear dichroism of $D \approx 1$ is resolved. Thus, the ability of the proposed measurement method to extract the effective parameters of samples with LB/CB/LD/CD is confirmed.

7 Conclusions and Discussions

This study has proposed a decoupled analytical technique based on the Mueller matrix method and the Stokes parameters for extracting LB, CB, LD, and CD properties of anisotropic optical

materials. The effective LB, CB, LD, and CD parameters of the sample are fully decoupled in the extraction process. Thus, the “multiple solutions” problem observed in Chen et al.³² and Lo et al.³³ when extracting the LB properties of a sample with a linear dichroism of $D \approx 1$ is resolved. In addition, the experimental results have shown that the decoupled nature of the extraction process localizes the effects of measurement errors and enables the properties of pure LB, LD, CB, or CD samples to be extracted without the need for any form of compensation process. As a result, the proposed approach has significant potential for applications such as collagen and muscle structure characterization (based on LB measurement only), protein structure characterization (based on CB/CD measurements), or diabetes detection (based on CB measurement only) without using a compensation technique or pretreatment. In contrast to existing analytical models based upon the Mueller matrix decomposition method, the six effective parameters are uniquely extracted in a totally decoupled manner. Also, the principal birefringence axis and diattenuation axis are not required to be aligned. Additionally, it is found that Eqs. (6)–(11) are all function of Mueller elements, thus those effective optical parameters also can be extracted by a Mueller polarimetry. Moreover, as similar to Sec. 3.2, the error bars of Mueller elements (m_{ij} , $i, j = 1 - 4$) obtained by Eqs. (6)–(11) have values less than ± 0.006 . As compared to ± 0.005 random perturbations in the output Stokes parameters, the extracted Mueller elements are still quite robust. Although only four different input polarization lights, namely three linear polarization lights (i.e., \hat{S}_0° , \hat{S}_{45° , and \hat{S}_{90°) and one circular polarization lights (i.e. \hat{S}_{RHC}) are enough in obtaining all Mueller elements. However, the over-determined system in obtaining all Mueller elements by using six input polarized

lights can provide an important means to verify the correctness of values extracted from the experimental results.

In future work, the proposed method will be extended in extracting nine effective parameters, not only on the orientation angle and phase retardance of LB, the orientation angle and linear dichroism of LD, the optical rotation of CB, and the circular dichroism of CD properties, but also on two linear depolarizations and the circular depolarization properties of turbid media.

Acknowledgments

The authors gratefully acknowledge the financial support provided to this study by the National Science Council of Taiwan under Grant No. NSC99-2221-E-006-034-MY3. Also, the related patent was issued in 2011.

References

- I. Tinoco, Jr., C. Bustamante, and M. F. Maestre, "The optical activity of nucleic acids and their aggregates," *Ann. Rev. Biophys. Bioeng.* **9**, 107–141 (1980).
- N. Berova, K. Nakanishi, and R. W. Woody, *Circular Dichroism: Principles and Applications*, Wiley-VCH, New York (2000).
- S. M. Kelly, T. J. Jess, and N. C. Price, "How to study proteins by circular dichroism," *Biochem. Biophys. Acta* **1751**(2), 119–139 (2005).
- N. A. Swords and B. A. Wallace, "Circular-dichroism analyses of membrane proteins: examination of environmental effects on bacteriorhodopsin spectra," *Biochem. J.* **289**(Pt. 1), 215–219 (1993).
- F. Zsila et al., "Circular dichroism and absorption spectroscopic data reveal binding of the natural cis-carotenoid bixin to human α_1 -acid glycoprotein," *Bioorg. Chem.* **33**(4), 298–309 (2005).
- H. Yao, T. Isohashi, and K. Kimura "Detection of spectral inhomogeneities of mesoscopic thiocyanine J aggregates in solution by the apparent CD spectral measurement," *Chem. Phys. Lett.* **419**(1–3), 21–27 (2005).
- E. Castiglioni, *CD Spectropolarimetry: The Instrumental Approach*, E. C. S, Italy (1999).
- C. Provenzano et al., "Method for artifact-free circular dichroism measurements based on polarization grating," *Opt. Lett.* **35**(11), 1822–1824 (2010).
- R. Kuroda, T. Harada, and Y. Shindo, "A solid-state dedicated circular dichroism spectrophotometer: development and application," *Rev. Sci. Instrum.* **72**(10), 3802–3810 (2001).
- T. Harada, H. Hayakawa, and R. Kuroda, "Vertical-type chiroptical spectrophotometer, (I): instrumentation and application to diffuse reflectance circular dichroism measurement," *Rev. Sci. Instrum.* **79**(7), 073103-1–073103-6 (2008).
- J. Kobayashi et al., "Optical properties of superconducting $\text{Bi}_2\text{Sr}_2\text{CaCu}_2\text{O}_8$," *Phys. Rev. B.* **53**(17), 11784–11795 (1996).
- J. Kobayashi and T. Asahi, "Development of HAUP and its applications to various kinds of solids," *Proc. SPIE* **4097**, 25–39 (2000).
- W. Kaminsky, K. Claborn, and B. Kahr, "Polarimetric imaging of crystals," *Chem. Soc. Rev.* **33**(8), 514–525 (2004).
- W. Kaminsky et al., "Optical rotatory and circular dichroic scattering," *J. Phys. Chem.* **107**(16), 2800–2807 (2003).
- K. Claborn et al., "Circular dichroism imaging microscopy: application to enantiomorphous twinning in biaxial crystals of 1,8-dihydroxyanthraquinone," *J. Am. Chem. Soc.* **125**(48), 14825–14831 (2003).
- D. B. Chenault and R. A. Chipman, "Measurements of linear diattenuation and linear retardance spectra with a rotating sample spectropolarimeter," *Appl. Opt.* **32**(19), 3513–3519 (1993).
- D. B. Chenault and R. A. Chipman, "Infrared birefringence spectra for cadmium-sulfide and cadmium selenide," *Appl. Opt.* **32**(22), 4223–4227 (1993).
- D. B. Chenault, R. A. Chipman, and S. Y. Lu, "Electro-optic coefficient spectrum of cadmium telluride," *Appl. Opt.* **33**(31), 7382–7389 (1994).
- E. A. Sornsin and R. A. Chipman, "Visible Mueller matrix spectropolarimetry," *Proc. SPIE* **3121**, 156–160 (1997).
- N. Ghosh, M. F. G. Wood, and I. A. Vitkin, "Mueller matrix decomposition for extraction of individual polarization parameters from complex turbid media exhibiting multiple scattering, optical activity, and linear birefringence," *J. Biomed. Opt.* **13**(4), 044036-14 (2008).
- M. F. G. Wood et al., "Proof-of-principle demonstration of a Mueller matrix decomposition method for polarized light tissue characterization in vivo," *J. Biomed. Opt.* **14**(1), 014029-5 (2009).
- N. Ghosh et al., "Mueller matrix decomposition for polarized light assessment of biological tissues," *J. Biophoton.* **2**(3), 145–156 (2009).
- N. Ghosh, M. F. G. Wood, and I. A. Vitkin, "Polarimetry in turbid, birefringent, optically active media: a Monte Carlo study of Mueller matrix decomposition in the backscattering geometry," *J. Appl. Phys.* **105**(10), 102023-8 (2009).
- X. Wang and L. V. Wang, "Propagation of polarized light in birefringent turbid media: a Monte Carlo study," *J. Biomed. Opt.* **7**(3), 279–290 (2002).
- X. R. Huang and R. W. Knighton, "Linear birefringence of the retinal nerve fiber layer measured in vitro with a multispectral imaging micro-polarimeter," *J. Biomed. Opt.* **7**(2), 199–204 (2002).
- X. R. Huang and R. W. Knighton, "Diattenuation and polarization preservation of retinal nerve fiber layer reflectance," *Appl. Opt.* **42**(28), 5737–5743 (2003).
- S. Y. Lu and R. A. Chipman, "Interpretation of Mueller matrices on polar decomposition," *J. Opt. Soc. Am. A* **13**(5), 1106–1113 (1996).
- R. M. A. Zazzam, "Propagation of partially polarized light through anisotropic media with or without depolarization: a differential 4×4 matrix calculus," *J. Opt. Soc. Am.* **68**(12), 1756–1767 (1978).
- R. Ossikovski, "Differential matrix formalism for depolarizing anisotropic media," *Opt. Lett.* **36**(12), 2330–2332 (2011).
- N. Ortega-Quijano and J. L. Arce-Diego, "Depolarizing differential Mueller matrices," *Opt. Lett.* **36**(13), 2429–2431 (2011).
- N. Ortega-Quijano and J. L. Arce-Diego, "Mueller matrix differential decomposition for direction reversal: application to samples measured in reflection and backscattering," *Opt. Exp.* **19**(15), 14348–14353 (2011).
- P. C. Chen et al., "Measurement of linear birefringence and diattenuation properties of optical samples using polarimeter and Stokes parameters," *Opt. Exp.* **17**(18), 15860–15884 (2009).
- Y. L. Lo, T. T. H. Pham, and P. C. Chen, "Characterization on five effective parameters of anisotropic optical material using Stokes parameters-Demonstration by a fiber-type polarimeter," *Opt. Exp.* **18**(9), 9133–9150 (2010).
- J. Morio and F. Goudail, "Influence of the order of diattenuator, retarder and polarizer in polar decomposition of Mueller matrices," *Opt. Lett.* **29**(19), 2234–2236 (2004).
- R. Ossikovski, "Interpretation of nondepolarizing Mueller matrices based on singular-value decomposition," *J. Opt. Soc. Am. A.* **25**(2), 473–482 (2008).
- S. N. Savenko and I. S. Marfin, "Invariance of anisotropy properties presentation in scope of polarization equivalence theorems," *Proc. SPIE* **6536**, 65360G-1–65360G-10 (2007).
- J. Schellman and H. P. Jensen, "Optical spectroscopy of oriented molecules," *Chem. Rev.* **87**(6), 1359–1399 (1987).
- O. Arteaga and A. Canillas, "Analytic inversion of the Mueller-Jones polarization matrices for homogeneous media," *Opt. Lett.* **35**(4), 559–561 (2010).
- N. Ghosh, M. F. G. Wood, and I. A. Vitkin, "Influence of the order of the constituent basis matrices on the Mueller matrix decomposition-derived polarization parameters in complex turbid media such as biological tissues," *Opt. Commun.* **283**(6), 1200–1208 (2010).
- F. Boulvert et al., "Decomposition algorithm of an experimental Mueller matrix," *Opt. Commun.* **282**(5), 692–704 (2009).
- Z. Michalewicz, *Genetic Algorithm + Data Structure = Evolution Programs*, Springer-Verlag, New York (1994).
- T. T. H. Pham, Y. L. Lo, and P. C. Chen, "Design of polarization-insensitive optical fiber probe based on effective optical parameters," *IEEE/OSA J. Light. Technol.* **29**(8), 1127–1135 (2011).
- Y. L. Lo and T. C. Yu, "Polarimetric glucose sensor using a liquid-crystal polarization modulator driven by a sinusoidal signal," *Opt. Commun.* **259**(1), 40–48 (2006).